Published in final edited form as:
Neuron. 2010 June 10; 66(5): 739–754. doi:10.1016/j.neuron.2010.04.029.

Deleterious Effects of Amyloid β Oligomers Acting as an Extracellular Scaffold for mGluR5

Marianne Renner[1,4], **Pascale N. Lacor**[2,4], **Pauline T. Velasco**[2], **Jian Xu**[3], **Anis Contractor**[3], **William L. Klein**[2,*], and **Antoine Triller**[1,*]

[1] Ecole Normale Supérieure, Institut de Biologie de l'Ecole Normale, Supérieure (IBENS) Paris France; Inserm U1024, Paris France; CNRS, UMR8197, 75005 Paris, France

[2] Neurobiology and Physiology Department, Northwestern University, Evanston, IL 60208, USA

[3] Department of Physiology, Northwestern University School of Medicine, Chicago, IL 60611, USA

SUMMARY

Soluble oligomers of amyloid β (Aβ) play a role in the memory impairment characteristic of Alzheimer's disease. Acting as pathogenic ligands, Aβ oligomers bind to particular synapses and perturb their function, morphology, and maintenance. Events that occur shortly after oligomer binding have been investigated here in live hippocampal neurons by single particle tracking of quantum dot-labeled oligomers and synaptic proteins. Membrane-attached oligomers initially move freely, but their diffusion is hindered markedly upon accumulation at synapses. Concomitantly, individual metabotropic glutamate receptors (mGluR5) manifest strikingly reduced lateral diffusion as they become aberrantly clustered. This clustering of mGluR5 elevates intracellular calcium and causes synapse deterioration, responses prevented by an mGluR5 antagonist. As expected, clustering by artificial crosslinking also promotes synaptotoxicity. These results reveal a mechanism whereby Aβ oligomers induce the abnormal accumulation and overstabilization of a glutamate receptor, thus providing a mechanistic and molecular basis for Aβ oligomer-induced early synaptic failure.

INTRODUCTION

Early Alzheimer's disease (AD) is distinguished by selective impairment of memory formation. The underlying mechanism putatively involves synaptic dysfunction and deterioration caused by soluble amyloid β oligomers, also referred to as ADDLs (Klein et al., 2001; Selkoe, 2002; Lacor, 2007). Aβ assembly additionally generates the insoluble fibrils found in Alzheimer's diagnostic amyloid plaques, which themselves constitute a source of Aβ oligomers (Aβo) in transgenic mouse AD models (Koffie et al., 2009). Aβo trigger various pathological traits associated with AD, such as tau hyperphosphorylation, production of reactive oxygen species, and selective neuronal death (references in Klein et al., 2007). Significantly for memory dysfunction, they rapidly alter synaptic plasticity, inhibiting long-term potentiation (LTP) (Lambert et al., 1998; Walsh et al., 2002; Townsend

*Correspondence: triller@biologie.ens.fr (A.T.), wklein@northwestern.edu (W.L.K.).
[4]These authors contributed equally to this work

SUPPLEMENTAL INFORMATION
Supplemental Information includes six figures, one movie, and Supplemental Experimental Procedures and can be found with this article online at doi:10.1016/j.neuron.2010.04.029.

et al., 2006) and facilitating long-term depression (LTD) (Wang et al., 2002; Hsieh et al., 2006; Shankar et al., 2008).

Aβo are gain-of-function pathogenic ligands that bind at membrane sites localized at particular synapses (Lacor et al., 2004). Timing of specific responses depends on the concentration and nature of the oligomers. In as little as 5 minutes, synthetic oligomers applied at relatively high concentrations bind at synapses and initiate pathological increases in the transcript of memory-related immediate early gene *arc* (Lacor et al., 2004). Anomalous spine morphology and depletion of surface NMDAR occur secondarily (Lacor et al., 2007). Application of metabolically produced oligomers at very low concentrations provokes a cofilin- and calcineurin-dependent decrease of NMDAR activity and dendritic spine number after 5 to 15 days (Shankar et al., 2007). Synapse loss, induced by Aβo in culture (Lacor et al., 2007) and in transgenic mouse AD models (Koffie et al., 2009), is thought to result from an initial excitotoxicity mediated by oxidative stress and increased intracellular Ca^{2+} (Ca^{2+}_i; Cullen et al., 1996; references in Bezprozvanny and Mattson, 2008). Aβo initially cause increased Ca^{2+}_i (Kelly and Ferreira, 2006; De Felice et al., 2007), which later diminishes with synapse loss (Shankar et al., 2007). Aberrant Ca^{2+} homeostasis and neuronal hyperexcitability occur in neurons that are close to Aβ plaques (Kuchibhotla et al., 2008; Busche et al., 2008), potentially involving Aβo-induced increased NMDAR responses and subsequent excitotoxicity (De Felice et al., 2007; Szegedi et al., 2005).

The specificity of Aβo binding requires membrane proteins that serve adventitiously as toxin receptors. A recently reported Aβo receptor is the cellular prion protein (PrPc). Anti-PrPc antibodies reduce binding of Aβo to the plasma membrane and rescue plasticity in hippocampal slices (Lauren et al., 2009). Binding of Aβo to lipid raft-bound PrPc raises the issue of their diffusion dynamics in the plasma membrane and the relation to synaptic physiology (Renner et al., 2009). Synaptic receptors are stabilized at the postsynaptic membrane by interactions with a subjacent meshwork of scaffolding proteins. Nevertheless, their stabilization is transient and receptors continuously diffuse in and out of the synaptic membrane (Triller and Choquet, 2008). Recent data on the dynamics of synaptic components supports the view of the synapse as a steady-state structure with different local equilibria that can be tuned to regulate receptor numbers at synapses (reviewed in Renner et al., 2008). In other words, the population of extrasynaptic receptors is in equilibrium with the synaptic one and interference with diffusion exchange rates is likely to modify synaptic efficacy (Ehlers et al., 2007).

We here propose a mechanism to explain the critical pathogenic ability of Aβo to reach synapses and hinder the distribution of memory-related receptors. Key results have come from experiments using single particle tracking (SPT) of Aβo labeled by quantum dots (QDs). We found in cultured mature hippocampal neurons that membrane-bound Aβo diffuse laterally and accumulate at excitatory synapses where they create clusters whose sizes increase with time. These pathological clusters greatly reduce the mobility of the group 1 metabotropic glutamate receptor 5 (mGluR5), which normally diffuses readily in the plasma membrane (Serge et al., 2002). As a consequence, mGluR5 aggregates in ectopic signaling platforms and impacts on calcium signaling and NMDAR amount at synapses. This effect was mimicked by artificial crosslinking of mGluR5 and inhibited by a specific antagonist. In hippocampal cultured neurons from mGluR5 knockout (KO) mice, Aβo binding to the neuronal surface was greatly reduced and the loss of NMDAR was almost abolished.

RESULTS

Interactions between Aβo and the surface membranes of living neurons were investigated by confocal fluorescence microscopy and by SPT analysis. The focus was on lateral diffusion properties of Aβo and different receptors for neurotransmitters shortly after Aβo attachment to cells (incubation times of up to 1 hr). Experiments used mature cultured hippocampal neurons [21–27 days in vitro (DIV)] and biotinylated (b-Aβo) or fluorescent Aβo prepared using methods previously described for unmodified Aβo (Klein, 2002). Such preparations are known to contain no fibrillar or protofibrillar assemblies and the oligomers that are present partition by HPLC into two fractions, with peaks near 60 kDa and 13 kDa (Chromy et al., 2003). The larger oligomers, previously shown to bind prominently to synaptic spines (Lacor et al., 2004, 2007), were obtained by cutoff filters (50 kDa) and used in most experiments described below (although, as noted, experiments with the smaller species suggested certain parallel properties). Fractionated or unfractionated oligomers all yielded predominantly tetramers, trimers, and monomers by SDS-PAGE (Figure S1A, available online). Larger oligomers, when initially prepared in vitro, thus are stable in aqueous buffer but break down into smaller species in the presence of SDS. As previously shown, these oligomers do not generate fibrils during incubation with neurons (Lacor et al., 2004). Aβo bind to the surface of neurons in a saturable dose-dependent manner (Figures S1B1–S1B2).

Aβ Oligomers Progressively Form Clusters at the Cell Surface

Confocal immunofluorescence microscopy has shown that Aβo cluster at synapses labeled with PSD95, NR1, and CaMKII (Lacor et al., 2004, 2007). We determined that their biotinylated counterparts (b-Aβo), detected by fluorescently labeled streptavidin, also preferentially associate with synapses. b-Aβo colocalized with Homer1b/c, a scaffolding protein concentrated at excitatory synapses that interacts with metabotropic glutamate receptors and members of the Shank family (Tu et al., 1999; Figures 1A–1C). On the contrary, b-Aβo showed little colocalization with the scaffolding protein of inhibitory synapses, Gephyrin, indicating the selective binding of Aβo to excitatory synapses (Figures 1A–1C).

In living neurons labeled with FM4-64 to identify active synapses, b-Aβo formed clusters comparable to those seen in fixed cells, with ~50% colocalizing or closely apposed to synapses (Figure 2A). The clusters became larger with increasing times of application (up to 60 min, t test $p < 0.0001$; Figure 2B), and their total fluorescence intensity increased nearly 4-fold (1.27-fold between 5 and 15 min and 3.73-fold between 5 and 60 min; t test $p < 0.0001$; Figure 2C). The fluorescence increase was more important at synaptic clusters (~20% more than at extrasynaptic clusters after 60 min, t test $p < 0.009$; Figure 2D). Because use of streptavidin to visualize the oligomers might potentially induce clustering, we also used Aβo coupled to tetramethyl-rhodamine (TAMRA-Aβo). Binding of TAMRA-Aβo gave the same oligomer distribution as seen with streptavidin (Figures S1C and S1D) and had similar synaptotoxicity (data not shown). In a “pulse-chase” experiment, TAMRA-Aβo was applied for 1 min at 100 nM. After 1 min of incubation, the TAMRA-Aβo had already formed clusters (Figure 2E) and ~50% of these clusters were associated with synapsin-stained presynaptic boutons. Observations from 1 to 10 min revealed that the fluorescence intensity of TAMRA-Aβo clusters increased progressively (Figures 2F and 2G). Their fluorescence was monitored after rinsing the neurons; therefore any change in the surface clustering of TAMRA-Aβo can only result from their reorganization by means of lateral diffusion.

Aβ Oligomers Show Time-Dependent Reduction of Lateral Diffusion

The physical properties of b-Aβo lateral diffusion were analyzed with SPT. Neurons were first treated with 500 nM b-Aβo for 5 or 60 min and then incubated with streptavidin-coupled QDs (Bannai et al., 2006; Figures S2A and S2B). Synapses were identified by labeling with FM4-64. QD labeling did not alter b-Aβo distribution between synaptic and extrasynaptic regions (~50% colocalized or apposed to FM4-64-positive puncta; Figures S2C and S2D). Single QDs, identified by their blinking, were detected with a pointing accuracy of 10–20 nm (Dahan et al., 2003). The movements of QD-bound Aβo (QD-Aβo) were tracked and their trajectories were reconstructed from 7.5 s stream recordings at 33 Hz (Figure S2B). The portions of trajectories that colocalized with FM spots were defined as synaptic. The diffusion coefficient D was derived from the initial slope of the mean square displacement (MSD) versus the time interval τ plot (MSD = 4Dτ). In our study, particles with D $<10^{-4}$ $\mu m^2 \cdot sec^{-1}$ were defined as immobile (<5% at both extrasynaptic and synaptic locations) and not analyzed further. The mean diffusive behavior, free or confined, was deduced from the shape of the average MSD versus τ curve. The trajectories of molecules diffusing with free (“Brownian”) diffusion display an MSD function that depends linearly on τ, while in case of confined motion it reaches a plateau (references in Triller and Choquet, 2008).

Lateral diffusion of QD-Aβo bound to plasma membranes was not constant, but decreased with time of exposure [60 min with respect to 5 min; Kolmogorov-Smirnov (KS) test, $p < 0.0001$ for trajectories outside as well as inside synapses; Table 1 and Figure 3A]. In harmony with these measurements, the MSD plots indicated a marked reduction in QD-Aβo mobility (Figure 3B). The clusters of b-Aβo also displayed small movements with values of D one or two orders of magnitude smaller than individual QD-Aβo (median D, 5 min: 4.85×10^{-4} $\mu m^2 \cdot sec^{-1}$, n = 856; 60 min: 5.19×10^{-4} $\mu m^2 \cdot sec^{-1}$, n = 1615). Neurons treated with b-Aβo at low concentration (20 nM) gave results analogous to those observed at 500 nM. An initial rapid diffusion dropped substantially by 60 min, both at extrasynaptic and synaptic sites (Figures 3C and 3D and Table 1), and the MSD plot displayed a similar time-dependent increase in confinement (Figures 3E and 3F). The SPT analysis together with the confocal fluorescence data imply that b-Aβo, bound to molecules diffusing in the membrane, undergo greatly decreased mobility as they accumulate within growing clusters. Interestingly, when low concentration b-Aβo were applied only briefly (5 min), analysis 1 hr later revealed that diffusion outside synapses was still high (5 + 60; median D: 3.08×10^{-2} $\mu m^2 \cdot sec^{-1}$, n = 107; Figures 3C and 3D). In contrast, oligomers inside synapses showed reduced mobility (median D: 0.91×10^{-2} $\mu m^2 \cdot sec^{-1}$, n = 96) as found with continuous application, suggesting that synaptic oligomers are more stabilized than the extrasynaptic ones.

We also investigated the characteristics of low-molecular-weight forms of Aβo (LMW-Aβo; <50 kDa). As with prior immunofluorescence observations (Lacor et al., 2007), LMW-Aβo were almost undetectable by streptavidin labeling (data not shown). However, it was possible to observe the nonabundantly bound LMW-Aβo by SPT, due to the higher sensitivity of this technique (Triller and Choquet, 2008). QD-LMW were found to diffuse faster than high-molecular-weight forms of Aβo (HMW-Aβo; >50 kDa) both inside and outside synapses (Figures S2E and S2F). Indeed, LMW-Aβo applied for 5 min at low concentration diffused similarly to any transmembrane protein at synaptic as well as at extrasynaptic locations. However, both high- and low-molecular-weight fractions were slowed down by increasing their concentration and/or the incubation length (Figures S2E and S2F). The possibility that these conditions foster reorganization of LMW-Aβo into larger oligomers cannot be ruled out. Overall, as expected in a diffusion process, the clustering of b-Aβo depends on the concentration and time of application; therefore, at low concentrations of oligomers more time is required to establish clusters.

Aβ Oligomers Redistribute mGluR5

The observed time-dependent reduction in Aβo mobility suggests their binding would alter the distribution and reduce the mobility of their associated proteins. There are a number of synaptic membrane molecules with which Aβo potentially interact. Several receptors and scaffolding proteins coimmunoprecipitated with Aβo in a detergent-stable complex released from synaptosomes (Figure 4A1); notably NMDAR subunits NR1 and NR2 and mGluR5 receptors. Consistent with this coimmunoprecipitation, an antibody against the extracellular termini of mGluR5 decreased the binding of Aβo to neurons (~42% reduction of fluorescence of Aβo puncta; Figure 4B1, ANOVA, $p < 0.001$), whereas antibodies directed against mGluR1 or mGluR2 had no effect (Figure 4B1). This reduction was dose dependent (Figure S3A) and occurred over a range of Aβo concentrations (31.25–500 nM; Figure S3B). No effect was seen after the preabsorption of antibody with a control antigen peptide (Figure S3C). Previous reports have shown similar inhibition of Aβo binding using antibodies raised against NR1 (De Felice et al., 2007) and PrPc (Lauren et al., 2009). Interestingly, incubation of neurons with combinations of antibodies did not increase the inhibition in comparison to the effect of individual antibodies (Figure S3C). This suggests that mGluR5, PrPc, and NR1 may be in proximity to each other as well as the Aβo binding site. Finally, the binding on hippocampal neurons cultured from *mGluR5*$^{-/-}$ and *mGluR5*$^{+/-}$ mice was reduced in a gene dosage-dependent manner to ~19% and ~47%, respectively, compared to wild-type mice (Figure 4B2 and Figure S3D), indicating that mGluR5 is implicated in the binding of Aβo.

To investigate whether Aβo may redistribute mGluR5s in cultured hippocampal neurons, we first measured the association of mGluR5 with oligomers in a Triton-resistant, DOC-extractable fraction. This approach was developed previously to obtain signal transduction complexes coupled to the spine cytoskeleton (Husi and Grant, 2001). Proteins were obtained from mature neurons incubated with different concentrations (52, 125, and 300 nM) of Aβo for 5 or 60 min (Figure 4A2). Western blot analysis showed a large increase of mGluR5 in the Triton-resistant fraction at 60 min, thus establishing the oligomer-dependent relocation of this receptor. A proportional relationship between mGluR5 receptors and oligomers was observed (linear regression $r^2 = 0.90$; data not shown), consistent with their coaccumulation.

The nature of the domain-comprising association of mGluR5 and Aβo was investigated using neurons transfected with a construct of mGluR5a tagged with Venus at its C terminus (mGluR5-Ve; Perroy et al., 2008). Without Aβo, mGluR5-Ve was equally dispersed between spines and dendritic shafts. The addition of HiLyte555-tagged Aβo (Hi-Aβo) promoted accumulation of mGluR5-Ve at dendritic spines. Fluorescence of the receptor was enriched in spines 1.3 and 2.5 times after 5 and 60 min, respectively (mean ± SEM; n = 194–776 spines on 25–43 cells; t test, $p < 0.0001$; Figures 4C and 4D1). The enrichment of mGluR5-Ve in spines was accompanied by increased Hi-Aβo fluorescence intensity (Figure 4D2 and Figure S3E).

Triple-label immunochemistry verified oligomer-induced recruitment of mGluR5 to synapses (Figures 4E–4G). Treatment with b-Aβo did not prevent the binding of an antibody targeting an extracellular epitope of mGluR5 (Figure 4E). By 5 min, clusters of b-Aβo and mGluR5 already showed a large degree of colocalization (44.63% ± 4.30%). This colocalization increased further by 60 min (60.06% ± 1.67%; n = 10 cells; t test, $p = 0.001$). The fluorescence intensity of mGluR5 clusters also increased in response to oligomer application [control: 460 ± 54 arbitrary units (a.u.), 5 min b-Aβo: 592 ± 21 a.u., 60 min b-Aβo: 748 ± 30 a.u.; t test, $p = 0.008$ and $p < 0.0001$, respectively; Figure 4F]. In these experiments, oligomers were added prior to fixation and processing for fluorescence microscopy, precluding any blockade of oligomer binding by the anti-mGluR5. Similar results were obtained using an antibody recognizing an intracellular epitope (Figure S3F).

As expected from the spine enrichment, there was an increase in the proportion of mGluR5 clusters occurring at synapses, which were labeled with anti-vGluT1. Only a minority of the mGluR5s were synaptic in nontreated neurons (35.22% ± 3.11%; Figures 4E–4G), and this distribution was unaltered by continued incubation with vehicle solution for b-Aβo (at 5 min: 36.13% ± 0.94%; t test, $p = 0.75$; at 60 min: 31.56% ± 0.96%; t test, $p = 0.13$) or by short exposure to b-Aβo (5 min; t test, $p = 0.98$). However, after 60 min exposure to Aβo, synaptic mGluR5 clusters increased significantly (53.69% ± 1.89%; t test, $p < 0.0001$; Figures 4E–4G). Interestingly, after a 5 min pulse of b-Aβo followed by a 60 min lag before observation, fluorescence intensity of mGluR5 clusters returned to control values (5 min b-Aβo + 60 min without b-Aβo: 432 ± 18 a.u.; t test, $p = 0.56$; Figure 4F) but localization of mGluRs was shifted to synapses (49.60% ± 2.18%; t test, $p < 0.0001$; Figure 4G). Overall, these data indicate that membrane-bound Aβo, by direct or indirect interactions, induce the dynamic redistribution of mGluR5 receptors to synapses.

Aβ Oligomers Reduce the Lateral Mobility of mGluR5

We next used SPT to analyze lateral diffusion of mGluR5, to test whether their redistribution induced by b-Aβo was associated with a change in receptor mobility. Treatment with b-Aβo did not prevent the subsequent binding to living neurons of the anti-mGluR5 antibody used for SPT (Figure 5A). It was shown that mGluR5 alternate between periods of fast and slow lateral diffusion, being slowed down over Homer clusters (Serge et al., 2002). As expected, we found that the diffusion of extrasynaptic QD-mGluR5 was faster than that at synaptic sites, identified by FM4-64 (Table 1, KS test, $p < 0.0001$). In dual-color SPT experiments, single QD-Aβo and QD-mGluR5 could be seen diffusing together (Movie S1).

Application of b-Aβo (500 nM) caused a striking, time-dependent increase in the proportion of slowly moving extrasynaptic mGluR5s, as indicated by a left shift of the D curve (Table 1 and Figure 5B). This shift in D value was accompanied by a major decrease in the explored surface area (Figure 5D, MSD plot). Even though diffusion remained Brownian (determined by the linear relationship between MSD and time interval), the explored surface area at 0.3–0.4 s dropped by 90% after 60 min [control: $186 \pm 6 \times 10^{-3}$ μm^2; 60 min: $19 \pm 1 \times 10^{-3}$ μm^2; Mann-Whitney (MW), $p < 0.0001$; n = 1782–1731]. After 5 min, the explored surface area was already reduced by 40% (5 min: $111 \pm 5 \times 10^{-3}$ μm^2; MW, $p < 0.0001$; n = 1809). The mobility of mGluR5 was also reduced at synapses, although the change was less drastic given their lower mobility in control conditions at this location (Table 1 and Figure 5C). The confinement increased in a time-dependent manner (Figure 5E) and the explored surface area decreased from $41 \pm 3 \times 10^{-3}$ μm^2 (control, n = 819) to $23 \pm 2 \times 10^{-3}$ μm^2 after 5 min (n = 678) and to 1 ± 10^{-3} μm^2 after 60 min (n = 735; MW, $p < 0.0001$). Similar results were obtained with 20 nM b-Aβo (Table 1). Overall, our results have shown that the progressive slowdown of Aβo diffusion was paralleled by a major decrease in mobility of mGluR5s.

The slower diffusion of mGluR5s was coupled with a reduced exchange of receptors between synaptic and extrasynaptic locations. In control conditions, ~70%–75% of synaptic receptors were exchanged during the recording period. After 60 min of application of b-Aβo (500 nM), the exchange was significantly reduced to 40%–45% (control: 73.43% ± 4.13%; b-Aβo 60 min: 43.53% ± 4.77%; t test, $p < 0.0001$). Decreased escape of receptors from synapses observed by SPT is consistent with the increased amount of synaptic mGluR5 seen by immunocytochemistry (see Figures 4D, 4E, and 4G).

In order to see whether the effect is independent from the labeling sequence, mGluR5 receptors were first labeled with QDs and observed in control conditions. The anti-mGluR5 antibody was used at a concentration (0.18 μg/ml) that did not prevent the binding of Aβo to cells (Figures S3A and S4C). After a sequence of recordings, Aβo were added to the

medium and mGluR5 mobility was followed on the same samples for the following 25 min. Receptors progressively slowed down at extra-synaptic and synaptic locations (Figures S4A–S4C) and some QD-mGluR5s were associated with Aβo clusters (Figure S4C). Thus the antibody-QD complex did not prevent the interaction of Aβo with the cell surface or the capacity of oligomers to cause slowdown and relocation of mGluR5 receptors.

Because the effect of b-Aβo on the mobility of mGluR5 could be due to a nonspecific action of oligomers on the membrane, we analyzed the lateral diffusion of AMPA-type glutamate receptors (AMPARs) and GABA receptors (GABARs). After 60 min of incubation, the mobility of AMPARs was not affected (Table 2 and Figures S4D and S4E). GABARs, however, were slowed down modestly at the extrasynaptic membrane but accelerated at synapses (Table 2 and Figures S4F and S4G).

Extracellular Scaffolding Alters Distribution and Mobility of mGluR5

The increased clustering and reduced mobility of mGluR5 caused by b-Aβo suggest that the latter could act as an “extra-cellular scaffold.” Indeed, a similar change in diffusive behavior could be produced by crosslinking receptors (X-link) using biotinylated antibodies and fluorescent streptavidin (Figure 6A). Crosslink-induced clusters of mGluR5 increased in fluorescence intensity with time (5 min: 131 ± 4 a.u.; 60 min: 233 ± 9 a.u.; t test, $p < 0.0001$), whereas there was no change in control fixed cells (Figure 6B). Their localization also was progressively shifted to synapses (5 min: 60.46% ± 1.86%; 60 min: 70.08% ± 2.04%; t test, $p = 0.002$; Figure 6C).

As expected, crosslinking significantly reduced the mobility of QD-mGluR5 (Figure 6D). The median D of extrasynaptic and synaptic QD-mGluR5 showed a large time-dependent decrease (~80%–90% by 60 min; Table 3). At the extrasynaptic membrane, the diffusion remained Brownian but the explored surface areas dropped significantly (Figure 6E). At synapses, the crosslinking increased the confinement of mGluR5 in a time-dependent manner (Figure 6E) and the exchange of receptors was reduced (control: 82% ± 5%; X-link: 50% ± 7%; t test, $p = 0.0006$). Specificity was indicated by the unchanged mobility of AMPAR at extrasynaptic as well as synaptic locations (Figures S5A and S5B). The results show that the scaffolding effect produced by crosslinking of mGluR5 recreates the effects of Aβo on the diffusion of receptors.

When crosslinking of mGluR5 was performed on neurons that were already treated with Aβo (nonbiotinylated ones, 20 nM), subsequent detection of Aβo by their antibody was impaired, but their mobility could still be detected by QD-coupled to anti-Aβo antibody. Importantly, the crosslinking of mGluR5 reduced the diffusion of QD-Aβo at both extrasynaptic and synaptic locations (Table 3 and Figure 6F). The reduction in mobility was also reflected on the MSD plot (Figure 6G). The data indicate that crosslinking of mGluR5 promotes the clustering of Aβo, analogous to the reciprocal effect instigated by Aβo.

Prevention of Aβ Oligomer-Induced Synaptic NMDAR (NR1) Loss by mGluR5 Antagonist and mGluR5 Knockout

The loss of NMDARs is one of the reported effects of long-lasting applications (more than 1 hr) of Aβ (Snyder et al., 2005) attributable to the presence of Aβo (Lacor et al., 2007). In the following experiments we made use of pure neuron cultures to prevent side effects caused by the action of Aβo on glial cells (Abramov and Duchen, 2005). As expected, exposure of neurons to b-Aβo (500 nM, 1 hr) reduced the fluorescence intensity of NR1 (Figures 7A and 7C). Most importantly, the Aβo-induced NR1 reduction was abolished when the neurons were pretreated with the specific mGluR5 noncompetitive antagonist SIB1757 (SIB), which negatively modulates the effect of agonists (Carroll, 2008; Figures 7A and 7C). In mGluR5

crosslinking experiments, NR1 was also reduced at synapses and SIB blocked the effect (Figures 7B and 7D). On the contrary, SIB did not alter the total fluorescence intensity of mGluR5 or that of Aβo clusters (data not shown). The results show that the Aβo-induced clustering of mGluR5, which is mimicked by the scaffolding effect of receptor antibody, has important functional consequences, producing an mGluR5 activity-dependent loss of NR1 immunoreactivity from the synaptic membrane. Experiments done on cultured neurons from mGluR5 KO mice reinforced the notion that the presence of mGluR5 was involved in the Aβo-induced loss of NMDAR. As previously reported (Wijetunge et al., 2008; She et al., 2009), *mGluR5*$^{+/-}$ and *mGluR5*$^{-/-}$ neurons expressed less NMDAR (~24% reduction; Figure 7E), but in *mGluR5*$^{-/-}$ mouse the loss of NR1 was nearly abolished. More precisely, after 3 hr of treatment with Aβo, NR1 labeling was reduced to ~20% and ~65% of control values on wild-type and *mGluR5*$^{+/-}$ neurons, respectively, and only to ~85% on *mGluR5*$^{-/-}$ neurons (Figure 7E).

Aβ Oligomers and mGluR5 Crosslinking Impact Intracellular Calcium and Network Activity

mGluR5 activity is known to elevate Ca^{2+}_i, a response also induced by Aβo in cultured neurons (Kelly and Ferreira, 2006; De Felice et al., 2007). We therefore carried out experiments to test the relationship between b-Aβo and mGluR5 and Ca^{2+}_i, using fluorescence intensity of Fluo-4 AM to monitor Ca^{2+}_i levels (Figures 8A and 8B). The total intensity, measured on a dendrite near to the cell body, was averaged during 2 s stream acquisitions at 5, 10, 15, and 30 min. Neurons that displayed a spontaneous increase in Ca^{2+}_i (transient or persistent) were counted as “responding” cells. In control conditions there were ~20% responding cells during the recorded session. After the addition of b-Aβo (500 nM, 5–30 min) the proportion of responding cells rose significantly (2.4-fold; Figure 8C). Importantly, this effect was abolished by an mGluR5 antagonist. When neurons were pretreated with SIB, the proportion of responding cells remained similar to that of control cells (Figure 8C). The Aβo-associated Ca^{2+}_i increase was time dependent and its amplitude in the remaining responding neurons was reduced after SIB treatment (Figure 8E). mGluR5 crosslinking experiments gave similar results (Figures 8D and 8F). Additionally, incubation with an antibody against the extracellular termini of mGluR5, which reduced Aβo binding to cells (Figure 4B), counteracted the rise of Ca^{2+}_i after 5 min of Aβo application (Figure 8G) and lowered the proportion of responding cells (Figure 8H). We also found no additive effects of Aβo treatment and crosslinking of mGluR5 on the Ca^{2+}_i increase at steady state, i.e., after 15 min of Aβo treatment (compare Figure 8G with Figures 8E and 8F), and the proportion of responding cells was similar to that of Aβo alone (Figures 8C and 8H). The nonadditivity of mGluR5 crosslinking and Aβo together with the inhibition of Aβo effects by anti-mGluR5 antibody strongly suggest a critical role for Aβo-mGluR5 interaction in mediating Aβo toxicity.

In a final experiment, the global effect of Aβo and the clustering of mGluR5 on synaptic activity was monitored with FM4-64 unloading. After synapses were loaded with FM4-64, the fluorescence decrease was monitored as a function of time following Aβo application (Figures S6A and S6B) or mGluR5 crosslinking (Figures S6C and S6D). As exemplified (Figures S6A and S6C) and quantified (Figures S6B and S6D), both treatments increased the FM4-64 unloading, an effect that was abolished by SIB. Taken together, the Ca^{2+}_i and FM4-64 experiments suggest that pathological clustering of mGluR5s caused by Aβo or mGluR5 crosslinking induces a network dysfunction that is preventable by the mGluR5 antagonist SIB.

DISCUSSION

We have investigated membrane protein dynamics following the initial binding of Aβo to neurons. Real-time analysis revealed three unsuspected events. First, Aβo formed clusters at

the synaptic plasma membrane in a manner that was time dependent. The binding was dependant on the presence of mGluR5. Second, the clustering altered the diffusion properties of mGluR5 receptors, which were redistributed within the plasma membrane. Third, and most significantly, the mGluR5 redistribution promoted an aberrant Ca^{2+} mobilization and loss of NMDAR. In essence, the creation of artificial signaling platforms by Aβo provides a mechanistic origin for synaptic chaos, the progressive dysfunction and degeneration that result in Alzheimer's memory loss.

Aβ Oligomers Diffuse Laterally and Progressively Create Clusters at the Neuronal Surface

Once bound to the membrane, Aβo progressively and rapidly built up clusters by means of lateral diffusion. The increasing size of the clusters was paralleled by reduced Aβo mobility. Comparable recruitment correlated with the reduction of diffusion is known for other membrane molecules including transmembrane proteins (Douglass and Vale, 2005). The kinetics of cluster formation depended on the concentration and time of application of Aβo, as expected for a diffusion-reaction process. The smaller oligomers, LMW-Aβo, applied at low concentration, diffused first similarly to any transmembrane protein but their diffusion slowed progressively with time. The effect was more rapid with HMW-Aβo, which also showed markedly higher overall binding affecting a higher proportion of synapses. We previously showed that HMW-Aβo triggered synaptotoxicity in 24 hr, while LMW-Aβo did not (Lacor et al., 2007), suggesting that a threshold in the amount of synaptic Aβo was not reached with the latter oligomers. The time and concentration dependence demonstrated here reconcile our results with those obtained by groups using various oligomer preparations (Hsieh et al., 2006; Shankar et al., 2007, 2008; Glabe, 2008; Lauren et al., 2009). Internalization of Aβo was not seen during the time course of our experiments, but this does not exclude the possibility that such a phenomenon may exist after longer incubation times, as seen by others (Saavedra et al., 2007). Long times (several hours) of treatment are needed to observe mitochondrial alterations and the timing depends on the conformation and concentration of Aβ (Deshpande et al., 2006).

Interactions of Aβo with the plasma membrane are not fully characterized. Preincubation of neurons with antibodies against NMDAR (De Felice et al., 2007), PrPc (Lauren et al., 2009), or mGluR5 (this study) decrease the binding of oligomers to the neuronal membrane, and Aβo might also bind to lipids (Sokolov et al., 2006). The implication of mGluR5 was further supported by the reduced Aβo binding on *mGluR5*$^{-/-}$ neurons. However, the binding was not totally abolished. Interestingly, our competition experiment with a cocktail of antibodies suggests that mGluR5, PrPc, and NMDAR are in proximity to each other. In fact, group 1 mGluRs are known to be part of large multimolecular complexes that contain NMDAR and possibly PrPc (Tu et al., 1999; Perroy et al., 2008; Khosravani et al., 2008).

Aβ Oligomers Redistribute mGluR5s and Affect Their Lateral Mobility

The fact that Aβo clusters recruit mGluR5 is of particular importance. mGluR5 is detected on dendrites mainly outside synapses. Synaptic mGluR5s form a ring at the periphery of the postsynaptic density (Lujan et al., 1997) where they are stabilized by the scaffolding Homer protein. Group 1 mGluRs are key participants in synaptic plasticity and excitotoxicity. They modulate NMDAR-dependent LTP and LTD in the hippocampus and participate in some forms of NMDAR-dependent learning (reviewed in Benarroch, 2008). Growing evidence supports the involvement of mGluR5 in the toxicity of Aβo. mGluR5 has also been reported to be involved in the modification of synaptic plasticity by Aβo (Wang et al., 2004), and recent studies have demonstrated that application of metabolically generated oligomers leads to a "mGluR-like" LTD of AMPARs (Hsieh et al., 2006). Actually, mGluR5-LTD depends on the immediate early gene Arc/Arg3.1 (Waung et al., 2008), which is rapidly elevated after exposure to Aβo (Lacor et al., 2004). mGluR5 also potentiates NMDAR-induced

excitotoxicity via a Ca^{2+}-activated PP2B/calcineurin activity (Bruno et al., 1995). Potentiation of NMDAR receptors provides an explanation for the ability of memantine, which therefore acts downstream from initiating events, to protect against aspects of Aβo toxicity (Lacor et al., 2007; De Felice et al., 2007). Interestingly, a study using organotypic cultures of brain slices has shown that calcineurin is needed for the synaptotoxicity of Aβo (Shankar et al., 2007). Finally, the second messenger cascade activated by mGluRs is involved, since oligomers decrease the amount of phosphatidylinositol diphosphate in a phospholipase C-dependent manner (Berman et al., 2008).

Once bound to the membrane, Aβo facilitate an increase in mGluR5 signaling associated with its dynamic redistribution to synapses. The Aβo-induced reduction of mGluR5 mobility was receptor specific because mobility of AMPARs and GABARs was not reduced at synapses. If anything, GABAR lateral diffusion was slightly accelerated. This paradoxical effect is probably related to the change in overall neuronal activity that was recently shown to underpin calcium-dependent regulation of inhibitory receptor lateral diffusion (Bannai et al., 2009). The crosslinking of mGluR5 by extracellular molecules (biotinylated antibodies and streptavidin) had effects similar to those of Aβo, suggesting that the latter act as an extracellular scaffold stabilizing mGluR5 and reducing its lateral diffusion.

Both Aβo and artificial crosslinking rapidly recruited mGluR5 to synapses, producing at the same time increased Ca^{2+}_i levels. Later there was a decrease in the number of synaptic NMDAR, which, as confirmed by experiments on *mGluR5*$^{-/-}$ neurons, was dependent on the presence of mGluR5. These synaptotoxic effects were prevented by the mGluR5 antagonist SIB, indicating a link between mGluR5 redistribution and increased signaling activity. A protective effect of this drug was also found in slices: SIB prevented LTD facilitation but not LTP inhibition following long-lasting application of Aβo (Shankar et al., 2008). Finally, receptors clustered outside synapses and being activated by glutamate spillover and glutamate release from astrocytes may also contribute to the abnormal signaling (Haydon and Carmignoto, 2006).

Aβ Oligomers as Inducers of Pathological Signaling Platforms

Our data show that the synaptotoxicity of Aβo relies, at least in part, on their capacity to alter the lateral diffusion of mGluR5 within the plasma membrane, thereby triggering disruptive signaling activity. Although the impact is selective for mGluR5 rather than AMPAR or GABAR, Aβo potentially could initiate additional toxic pathways by modifying the lateral dynamics of other membrane proteins. Aβo, for example, may also interact with molecules such as the voltage-gated calcium channel (Nimmrich et al., 2008), the angiotensin II receptor (Abdalla et al., 2008), or the acetylcholine receptors (Dougherty et al., 2003; Liu et al., 2009).

Current results support the concept that mGluR5 may provide a better target for pharmacological treatment in AD than NMDARs, which are downstream in the synaptotoxic pathway. Additionally, the pathogenic mechanism that we have identified here implies that identifying compounds that block clustering of membrane-bound Aβo might pave the way for alternative or complementary therapeutic approaches.

EXPERIMENTAL PROCEDURES

Cell Culture and Transfection

Hippocampal neurons from 18-day-old Sprague-Dawley rat embryos or P1 pups from mGluR5 KO mice (Xu et al., 2009) were cultured as explained in the Supplemental Information. In the case of transfection with Venus-tagged mGluR5a (Perroy et al., 2008), neurons were transfected at 9 DIV using Lipofectamine 2000 (Invitrogen) following the

manufacturer's instructions. Mature neuronal cultures (21–27 DIV), which have completed synaptic maturation, were used in all experiments. Rats were used in accordance with Animal Care and Use Committee institutional and national guidelines and regulations for approved protocols.

Unmodified and Modified Aβ Oligomer (ADDL) Preparations

Synthetic Aβo were prepared according to published protocols (Supplemental Information) using unmodified or tagged Aβ1-42 peptides: N terminus biotin tagged (American Peptide) or TAMRA, FAM, or HiLyte555 labeled (AnaSpec). Unless noted, experiments used b-Aβo retained by a 50 kDa cutoff filter. Aβo concentrations indicated refer to Aβ monomer equivalent.

Antibodies and Quantification of Fluorescence on Fixed Neurons

The primary antibodies used to recognize post-synaptic densities were monoclonal anti-gephyrin (mAb7a; Alexis Biochemicals) and polyclonal anti-Homer1b/c (Synaptic Systems). Aβo were detected with monoclonal NU1 or NU2 (Lambert et al., 2007). mGluR5 was detected using rabbit polyclonal antibodies directed against extracellular (Alomone Labs) or intracellular epitopes (Millipore). AMPAR and NMDAR were detected using mouse monoclonal anti-GluR2 or anti-NR1 (BD Biosciences), respectively. Other antibodies were anti-γ2 for GABAR (as in Bannai et al., 2009) and anti-mGluR1 (rabbit polyclonal; Alomone), anti-mGluR2 (Santa Cruz Biotechnology), monoclonal anti-streptavidin (Abcam), anti-vGluT1 (guinea pig polyclonal; Millipore), and anti-synapsin (Synaptic Systems). Secondary antibodies were FITC-, Cy3-, and Cy5-conjugated goat anti-mouse, anti-rabbit, or anti-guinea pig (highly cross-reacted; Jackson ImmunoResearch). Alternatively, biotinylated proteins were detected using Alexa 488-, Alexa 555-, or Alexa 647-conjugated streptavidin (Invitrogen).

Immunocytochemistry experiments are detailed in Supplemental Information and in Lacor et al. (2007). The immunolabeling of surface membrane proteins was performed in nonpermeabilizing conditions. Imaging was performed on a spinning disk confocal microscope (Leica DM5000B; Leica Microsystems; spinning disk head, Yokogawa CSU10; Yokogawa) or a Leica TCS SP2 Laser confocal microscope. The whole systems were driven by Metamorph software (Molecular Devices). In case of mGluR5-Ve-transfected neurons, 15–25 regions were chosen on top or outside spines. A stack of images separated 200 nm in the z axis was taken for each wavelength (Venus and HiLyte555). Fluorescence was corrected by subtracting background intensity. Quantification was made choosing the four to five planes with maximum Venus intensity and averaging the fluorescence of these planes for each wavelength. The enrichment of mGluR5-Ve in spines was calculated by dividing the fluorescence intensity of each spine by the mean fluorescence intensity outside spines on the same cell. In other cases, images were filtered by segmentation and wavelet transformation (see Supplemental Information) and quantitative analyses (size and total intensity) of the resulting synaptic puncta were done using the "integrated morphometry" feature of Metamorph v7.5. Colocalization and/or apposition between the puncta of two images were determined using one of the images as a mask. For this purpose, the puncta of the mask were expanded in one pixel (95 nm).

Aβ Oligomer Binding

Neurons were incubated for the indicated times with Aβo (unmodified, biotinylated, or fluorescently tagged) diluted in culture medium to the indicated concentrations. Control neurons were incubated with the same amount of vehicle solution added to the culture medium. Cells were rinsed twice with MEM recording medium (MEMr; phenol red-free MEM, 33 mM glucose, 20 mM HEPES, 2 mM glutamine, 1 mM sodium-pyruvate, and 1×

B27) and used for SPT or immunocytochemistry experiments. When streptavidin was used to reveal the localization of Aβo, neurons were incubated for 5 min with the fluorescent streptavidin solution (0.25 μM in MEMr) added immediately after rinsing. Blocking of Aβo hot-spot binding was performed by incubating neurons for 15 min with 5 μg/ml of antibodies directed to extracellular epitopes (N-ter) prior to 15 min Aβo treatment. Antibodies used were anti-mGluR5, anti-mGluR1, and anti-mGluR2 or anti-mGluR5 preadsorbed with the control antigen.

Coisolation of Synaptic Proteins and Aβ Oligomers

The coisolation of synaptic proteins and Aβo from synaptosomes was performed as previously described (Lacor et al., 2007; see Supplemental Information). The kinetics of mGluR5 and Aβo coisolation was investigated in the Triton-resistant DOC-extractable fraction of hippocampal neurons in cultures. After treatment of 21 DIV hippocampal cell cultures with Aβo or vehicle at different concentration (52, 125, and 300 nM) for various times (5 and 60 min) at 37°C in conditioned media, cells were washed and subsequently incubated with anti-Aβo NU-2. Isolation protocol is detailed in Supplemental Information. Lysates and immunoprecipitates were analyzed by western blot using anti-mGluR5 or anti-Aβo NU-1.

Crosslinking of mGluR5

In crosslinking experiments, neurons were first incubated with a primary antibody directed against the extracellular terminus of mGluR5 (10′, 7.5 μg/ml) and then with the corresponding biotinylated $F(ab')_2$ fragment (10′; Jackson ImmunoResearch). Cells were then incubated with Alexa 488-streptavidin diluted in MEMr (0.25 μM) for the indicated periods of time. Control neurons were incubated only with the primary antibody and Alexa 488-streptavidin or with the primary antibody preadsorbed with the mGluR5 control antigen. No staining by streptavidin was observed in these conditions.

Quantum Dot Labeling of Aβ Oligomers and Receptors for Single Particle Imaging

Neurons incubated with b-Aβo were incubated for 1 min with streptavidin-coated QDs emitting at 605 nm (0.2–0.3 nM; Invitrogen) as in Bannai et al. (2006). To track the movement of receptors or unmodified Aβo, QDs emitting at 605 nm conjugated with goat $F(ab')_2$ anti-rabbit or anti-mouse IgG (Invitrogen) were previously coupled with the corresponding primary antibody directed to extracellular epitopes of the receptors (anti-GluR2, anti-GABA γ2, or anti-mGluR5) or anti-Aβo NU1. QDs were incubated first with the antibody (6:1 molar ratio, 30 min) and then for an additional 15 min with casein to block nonspecific binding. Cells were incubated for 10 min at 37°C with the precoupled QDs and rinsed. Synapses were labeled with FM4-64 (15 s in a solution with FM and 40 mM KCl). All incubation steps and washes were performed at 37°C. Cells were imaged within 30 min after QD staining. When SPT of Aβo was performed after mGluR5 crosslinking, neurons were first incubated with unmodified Aβo (20 nM) for 5 min and then mGluR5 was cross-linked as described above.

Single Particle Tracking and Lateral Diffusion Analysis

Neurons were imaged in the MEMr at 37°C in an open chamber mounted on an IX70 inverted microscope (Olympus) as described in Renner et al. (2009). Single QDs were identified by their blinking (Dahan et al., 2003). Synaptic stain images were filtered by segmentation and wavelet transformation (references in Renner et al., 2009). Trajectories were defined as synaptic if they colocalized with a synaptic cluster or if they were in a "perisynaptic" ring of two pixels (~400 nm) around the synaptic cluster. Tracking was performed with homemade software in MatLab (The Mathworks). The center of the spot

fluorescence was determined by Gaussian fit with a spatial resolution of ~10–20 nm. Tracking of Aβo clusters was performed identifying them as for synaptic clusters. In this case, the spatial resolution was ~30 nm. The spots in a given frame were associated with the maximum likely trajectories estimated on previous frames of the image sequence. Only trajectories with at least 15 consecutive frames were used. The MSD was calculated using $MSD(ndt) = (N - n)^{-1}\Sigma_{i=1}^{N-n}[(x_{i+n} - x_i)^2 + (y_{i+n} - y_i)^2]$, where x_i and y_i are the coordinates of an object on frame *i*, *N* is the total number of steps in the trajectory, *dt* is the time between two successive frames, and *ndt* is the time interval over which displacement is averaged (Triller and Choquet, 2008). The diffusion coefficient D was calculated by fitting the first 2 to 5 points of the MSD plot versus time with the equation $MSD(t) = 4D_{2-5}t + 4\sigma_x^2$, with σ_x as the spot localization accuracy in one direction (references in Renner et al., 2009). Due to the large dispersal of values of D, we compared the median values. The explored surface area between 0.3 and 0.4 s corresponds to the average MSD for the mentioned intervals. The percentage of exchange was calculated as the proportion of trajectories that exit synaptic areas at least once during the recording session.

Ca^{2+} Imaging

Neurons (pure neuron cultures) were loaded with 0.5 μM Fluo-4 AM for 5 min at 37°C in MEMr and incubated for an additional 5 min in imaging medium to allow complete de-esterification of the intracellular AM esters. Fluo4 AM fluorescence was monitored before the treatment (time 0) and at 5, 10, 15, and 30 min after adding the corresponding drugs. When SIB (Tocris) was used, neurons were incubated for 30 min before the experiment with the drug diluted in culture medium (3 μM). After the experiments, cells were labeled with Alexa 555-conjugated streptavidin to assess Aβo binding. The imaging was performed at 37°C under an inverted Leica DM-IRB microscope equipped with a 63× objective (NA 1.32), a cooled CCD camera (CoolSNAP; Roper Scientific), and appropriate filters (for Fluo4 AM, excitation: 500 ± 20 nm; emission: 535 ± 30 nm; for FM excitation: 535 ± 50 nm, emission: from 590 nm). At each time point, the image acquisition consisted of a 20 frame stream recording, which was averaged to obtain one image used for quantifications. The total fluorescence intensity was measured on one region per cell, chosen inside a dendrite close to the cell body. The ratio of the fluorescence intensities in comparison with the initial values (F/Fo) was calculated after subtraction of the background fluorescence. If the fluorescence increased more than 10%, the cell was considered as a “responding” cell.

Statistical Analysis and Image Preparation

Unless noted, statistical analyses were done using Prism software (GraphPad Software) or built-in functions in MatLab using a two-tailed Student’s t test, the MW, KS, or ANOVA tests (Newman-Keuls or Tukey’s comparison tests). Data was obtained from at least three independent experiments. Image analysis was performed using Metamorph software (Molecular Devices) or ImageJ software (http://rsbweb.nih.gov/ij/). Images were prepared using Photoshop (Adobe Systems).

Supplementary Material

Refer to Web version on PubMed Central for supplementary material.

Acknowledgments

P.N.L., P.T.V, and W.L.K were supported by Alzheimer’s Association IIRG-06-26989, American Health Association A2006-092, and National Institutes of Health RO1AG029460, and partially by the Nanoscale Science and Engineering Initiative of the National Science Foundation (NSF) under NSF Award Number EEC-06475560. Thanks to C. Mirkin for attributing to P.N.L an international travel grant under the NSF Award mentioned above. The authors thank A. Wadhwani and R. Sureka for their help with the biochemistry experiments. M.R. was

supported by the Agence Nationale de la Recherche grant Neur-043-02. This research was partially funded by the Fondation pour la Recherche Médicale. We thank L. Fagni (Montpellier, France) for kindly provide us with the construct of mGluR5-Venus. W.L.K. is cofounder of Acumen Pharmaceuticals, licensed by Northwestern to develop Alzheimer's therapeutics and diagnostics that target ADDLs.

References

Abdalla S, Lother H, El Missiry A, Langer A, Sergeev P, El Faramawy Y, Quitterer U. Angiotensin II AT2 receptor oligomers mediate G-protein dysfunction in an animal model of Alzheimer disease. J Biol Chem. 2008; 284:6554–6565. [PubMed: 19074441]

Abramov AY, Duchen MR. The role of an astrocytic NADPH oxidase in the neurotoxicity of amyloid beta peptides. Philos Trans R Soc Lond B Biol Sci. 2005; 360:2309–2314. [PubMed: 16321801]

Bannai H, Levi S, Schweizer C, Dahan M, Triller A. Imaging the lateral diffusion of membrane molecules with quantum dots. Nat Protoc. 2006; 1:2628–2634. [PubMed: 17406518]

Bannai H, Levi S, Schweizer C, Inoue T, Launey T, Racine V, Sibarita JB, Mikoshiba K, Triller A. Activity-dependent tuning of inhibitory neurotransmission based on GABAAR diffusion dynamics. Neuron. 2009; 62:670–682. [PubMed: 19524526]

Benarroch EE. Metabotropic glutamate receptors: synaptic modulators and therapeutic targets for neurologic disease. Neurology. 2008; 70:964–968. [PubMed: 18347319]

Berman DE, Dall'Armi C, Voronov SV, McIntire LB, Zhang H, Moore AZ, Staniszewski A, Arancio O, Kim TW, Di Paolo G. Oligomeric amyloid-beta peptide disrupts phosphatidylinositol-4,5-bisphosphate metabolism. Nat Neurosci. 2008; 11:547–554. [PubMed: 18391946]

Bezprozvanny I, Mattson MP. Neuronal calcium mishandling and the pathogenesis of Alzheimer's disease. Trends Neurosci. 2008; 31:454–463. [PubMed: 18675468]

Bruno V, Copani A, Knopfel T, Kuhn R, Casabona G, Dell'Albani P, Condorelli DF, Nicoletti F. Activation of metabotropic glutamate receptors coupled to inositol phospholipid hydrolysis amplifies NMDA-induced neuronal degeneration in cultured cortical cells. Neuropharmacology. 1995; 34:1089–1098. [PubMed: 8532158]

Busche MA, Eichhoff G, Adelsberger H, Abramowski D, Wiederhold KH, Haass C, Staufenbiel M, Konnerth A, Garaschuk O. Clusters of hyperactive neurons near amyloid plaques in a mouse model of Alzheimer's disease. Science. 2008; 321:1686–1689. [PubMed: 18802001]

Carroll FI. Antagonists at metabotropic glutamate receptor subtype 5: structure activity relationships and therapeutic potential for addiction. Ann N Y Acad Sci. 2008; 1141:221–232. [PubMed: 18991960]

Chromy BA, Nowak RJ, Lambert MP, Viola KL, Chang L, Velasco PT, Jones BW, Fernandez SJ, Lacor PN, Horowitz P, et al. Self-assembly of Abeta(1-42) into globular neurotoxins. Biochemistry. 2003; 42:12749–12760. [PubMed: 14596589]

Cullen WK, Wu J, Anwyl R, Rowan MJ. beta-Amyloid produces a delayed NMDA receptor-dependent reduction in synaptic transmission in rat hippocampus. Neuroreport. 1996; 8:87–92. [PubMed: 9051758]

Dahan M, Levi S, Luccardini C, Rostaing P, Riveau B, Triller A. Diffusion dynamics of glycine receptors revealed by single-quantum dot tracking. Science. 2003; 302:442–445. [PubMed: 14564008]

De Felice FG, Velasco PT, Lambert MP, Viola K, Fernandez SJ, Ferreira ST, Klein WL. Abeta oligomers induce neuronal oxidative stress through an N-methyl-D-aspartate receptor-dependent mechanism that is blocked by the Alzheimer drug memantine. J Biol Chem. 2007; 282:11590–11601. [PubMed: 17308309]

Deshpande A, Mina E, Glabe C, Busciglio J. Different conformations of amyloid beta induce neurotoxicity by distinct mechanisms in human cortical neurons. J Neurosci. 2006; 26:6011–6018. [PubMed: 16738244]

Dougherty JJ, Wu J, Nichols RA. Beta-amyloid regulation of presynaptic nicotinic receptors in rat hippocampus and neocortex. J Neurosci. 2003; 23:6740–6747. [PubMed: 12890766]

Douglass AD, Vale RD. Single-molecule microscopy reveals plasma membrane microdomains created by protein-protein networks that exclude or trap signaling molecules in T cells. Cell. 2005; 121:937–950. [PubMed: 15960980]

Ehlers MD, Heine M, Groc L, Lee MC, Choquet D. Diffusional trapping of GluR1 AMPA receptors by input-specific synaptic activity. Neuron. 2007; 54:447–460. [PubMed: 17481397]

Glabe CG. Structural classification of toxic amyloid oligomers. J Biol Chem. 2008; 283:29639–29643. [PubMed: 18723507]

Haydon PG, Carmignoto G. Astrocyte control of synaptic transmission and neurovascular coupling. Physiol Rev. 2006; 86:1009–1031. [PubMed: 16816144]

Hsieh H, Boehm J, Sato C, Iwatsubo T, Tomita T, Sisodia S, Malinow R. AMPAR removal underlies Abeta-induced synaptic depression and dendritic spine loss. Neuron. 2006; 52:831–843. [PubMed: 17145504]

Husi H, Grant SG. Isolation of 2000-kDa complexes of N-methyl-D-aspartate receptor and postsynaptic density 95 from mouse brain. J Neurochem. 2001; 77:281–291. [PubMed: 11279284]

Kelly BL, Ferreira A. beta-Amyloid-induced dynamin 1 degradation is mediated by N-methyl-D-aspartate receptors in hippocampal neurons. J Biol Chem. 2006; 281:28079–28089. [PubMed: 16864575]

Khosravani H, Zhang Y, Tsutsui S, Hameed S, Altier C, Hamid J, Chen L, Villemaire M, Ali Z, Jirik FR, Zamponi GW. Prion protein attenuates excitotoxicity by inhibiting NMDA receptors. J Cell Biol. 2008; 181:551–565. [PubMed: 18443219]

Klein WL. Abeta toxicity in Alzheimer's disease: globular oligomers (ADDLs) as new vaccine and drug targets. Neurochem Int. 2002; 41:345–352. [PubMed: 12176077]

Klein WL, Krafft GA, Finch CE. Targeting small Abeta oligomers: the solution to an Alzheimer's disease conundrum? Trends Neurosci. 2001; 24:219–224. [PubMed: 11250006]

Klein, WL.; Lacor, PN.; De Felice, FG.; Ferreira, ST. IPSEN Fondation. Molecules that disrupt memory circuits in Alzheimer's disease: the attack on synapses by Abeta oligomers (ADDLs). In: Bontempi, B.; Silva, A.; Christen, Y., editors. Memories: Molecules and Circuits. Paris, France: Springer-Verlag; 2007.

Koffie RM, Meyer-Luehmann M, Hashimoto T, Adams KW, Mielke ML, Garcia-Alloza M, Micheva KD, Smith SJ, Kim ML, Lee VM, et al. Oligomeric amyloid β associates with postsynaptic densities and correlates with excitatory synapse loss near senile plaques. Proc Natl Acad Sci USA. 2009; 106:4012–4017. [PubMed: 19228947]

Kuchibhotla KV, Goldman ST, Lattarulo CR, Wu HY, Hyman BT, Bacskai BJ. Abeta plaques lead to aberrant regulation of calcium homeostasis in vivo resulting in structural and functional disruption of neuronal networks. Neuron. 2008; 59:214–225. [PubMed: 18667150]

Lacor PN. Advances in the understanding of the origins of synaptic pathology in AD. Curr Genomics. 2007; 8:486–508. [PubMed: 19415125]

Lacor PN, Buniel MC, Chang L, Fernandez SJ, Gong Y, Viola KL, Lambert MP, Velasco PT, Bigio EH, Finch CE, et al. Synaptic targeting by Alzheimer's-related amyloid beta oligomers. J Neurosci. 2004; 24:10191–10200. [PubMed: 15537891]

Lacor PN, Buniel MC, Furlow PW, Clemente AS, Velasco PT, Wood M, Viola KL, Klein WL. Abeta oligomer-induced aberrations in synapse composition, shape, and density provide a molecular basis for loss of connectivity in Alzheimer's disease. J Neurosci. 2007; 27:796–807. [PubMed: 17251419]

Lambert MP, Barlow AK, Chromy BA, Edwards C, Freed R, Liosatos M, Morgan TE, Rozovsky I, Trommer B, Viola KL, et al. Diffusible, nonfibrillar ligands derived from Abeta1-42 are potent central nervous system neurotoxins. Proc Natl Acad Sci USA. 1998; 95:6448–6453. [PubMed: 9600986]

Lambert MP, Velasco PT, Chang L, Viola KL, Fernandez S, Lacor PN, Khuon D, Gong Y, Bigio EH, Shaw P, et al. Monoclonal antibodies that target pathological assemblies of Abeta. J Neurochem. 2007; 100:23–35. [PubMed: 17116235]

Lauren J, Gimbel DA, Nygaard HB, Gilbert JW, Strittmatter SM. Cellular prion protein mediates impairment of synaptic plasticity by amyloid-beta oligomers. Nature. 2009; 457:1128–1132. [PubMed: 19242475]

Liu Q, Huang Y, Xue F, Simard A, DeChon J, Li G, Zhang J, Lucero L, Wang M, Sierks M, et al. A novel nicotinic acetylcholine receptor subtype in basal forebrain cholinergic neurons with high sensitivity to amyloid peptides. J Neurosci. 2009; 29:918–929. [PubMed: 19176801]

Lujan R, Roberts JD, Shigemoto R, Ohishi H, Somogyi P. Differential plasma membrane distribution of metabotropic glutamate receptors mGluR1 alpha, mGluR2 and mGluR5, relative to neurotransmitter release sites. J Chem Neuroanat. 1997; 13:219–241. [PubMed: 9412905]

Nimmrich V, Grimm C, Draguhn A, Barghorn S, Lehmann A, Schoemaker H, Hillen H, Gross G, Ebert U, Bruehl C. Amyloid beta oligomers (A beta(1-42) globulomer) suppress spontaneous synaptic activity by inhibition of P/Q-type calcium currents. J Neurosci. 2008; 28:788–797. [PubMed: 18216187]

Perroy J, Raynaud F, Homburger V, Rousset MC, Telley L, Bockaert J, Fagni L. Direct interaction enables cross-talk between ionotropic and group I metabotropic glutamate receptors. J Biol Chem. 2008; 283:6799–6805. [PubMed: 18182392]

Renner M, Specht CG, Triller A. Molecular dynamics of post-synaptic receptors and scaffold proteins. Curr Opin Neurobiol. 2008; 18:532–540. [PubMed: 18832033]

Renner M, Choquet D, Triller A. Control of the postsynaptic membrane viscosity. J Neurosci. 2009; 29:2926–2937. [PubMed: 19261888]

Saavedra L, Mohamed A, Ma V, Kar S, de Chaves EP. Internalization of beta-amyloid peptide by primary neurons in the absence of apolipoprotein E. J Biol Chem. 2007; 282:35722–35732. [PubMed: 17911110]

Selkoe DJ. Alzheimer's disease is a synaptic failure. Science. 2002; 298:789–791. [PubMed: 12399581]

Serge A, Fourgeaud L, Hemar A, Choquet D. Receptor activation and homer differentially control the lateral mobility of metabotropic glutamate receptor 5 in the neuronal membrane. J Neurosci. 2002; 22:3910–3920. [PubMed: 12019310]

Shankar GM, Bloodgood BL, Townsend M, Walsh DM, Selkoe DJ, Sabatini BL. Natural oligomers of the Alzheimer amyloid-beta protein induce reversible synapse loss by modulating an NMDA-type glutamate receptor-dependent signaling pathway. J Neurosci. 2007; 27:2866–2875. [PubMed: 17360908]

Shankar GM, Li S, Mehta TH, Garcia-Munoz A, Shepardson NE, Smith I, Brett FM, Farrell MA, Rowan MJ, Lemere CA, et al. Amyloid-beta protein dimers isolated directly from Alzheimer's brains impair synaptic plasticity and memory. Nat Med. 2008; 14:837–842. [PubMed: 18568035]

She WC, Quairiaux C, Albright MJ, Wang YC, Sanchez DE, Chang PS, Welker E, Lu HC. Roles of mGluR5 in synaptic function and plasticity of the mouse thalamocortical pathway. Eur J Neurosci. 2009; 29:1379–1396. [PubMed: 19519626]

Snyder EM, Nong Y, Almeida CG, Paul S, Moran T, Choi EY, Nairn AC, Salter MW, Lombroso PJ, Gouras GK, Greengard P. Regulation of NMDA receptor trafficking by amyloid-beta. Nat Neurosci. 2005; 8:1051–1058. [PubMed: 16025111]

Sokolov Y, Kozak JA, Kayed R, Chanturiya A, Glabe C, Hall JE. Soluble amyloid oligomers increase bilayer conductance by altering dielectric structure. J Gen Physiol. 2006; 128:637–647. [PubMed: 17101816]

Szegedi V, Juhasz G, Budai D, Penke B. Divergent effects of Abeta1-42 on ionotropic glutamate receptor-mediated responses in CA1 neurons in vivo. Brain Res. 2005; 1062:120–126. [PubMed: 16248989]

Townsend M, Shankar GM, Mehta T, Walsh DM, Selkoe DJ. Effects of secreted oligomers of amyloid beta-protein on hippocampal synaptic plasticity: a potent role for trimers. J Physiol. 2006; 572:477–492. [PubMed: 16469784]

Triller A, Choquet D. New concepts in synaptic biology derived from single-molecule imaging. Neuron. 2008; 59:359–374. [PubMed: 18701063]

Tu JC, Xiao B, Naisbitt S, Yuan JP, Petralia RS, Brakeman P, Doan A, Aakalu VK, Lanahan AA, Sheng M, Worley PF. Coupling of mGluR/Homer and PSD-95 complexes by the Shank family of postsynaptic density proteins. Neuron. 1999; 23:583–592. [PubMed: 10433269]

Walsh DM, Klyubin I, Fadeeva JV, Cullen WK, Anwyl R, Wolfe MS, Rowan MJ, Selkoe DJ. Naturally secreted oligomers of amyloid beta protein potently inhibit hippocampal long-term potentiation in vivo. Nature. 2002; 416:535–539. [PubMed: 11932745]

Wang HW, Pasternak JF, Kuo H, Ristic H, Lambert MP, Chromy B, Viola KL, Klein WL, Stine WB, Krafft GA, Trommer BL. Soluble oligomers of beta amyloid (1-42) inhibit long-term potentiation

but not long-term depression in rat dentate gyrus. Brain Res. 2002; 924:133–140. [PubMed: 11750898]

Wang Q, Walsh DM, Rowan MJ, Selkoe DJ, Anwyl R. Block of long-term potentiation by naturally secreted and synthetic amyloid beta-peptide in hippocampal slices is mediated via activation of the kinases c-Jun N-terminal kinase, cyclin-dependent kinase 5, and p38 mitogen-activated protein kinase as well as metabotropic glutamate receptor type 5. J Neurosci. 2004; 24:3370–3378. [PubMed: 15056716]

Waung MW, Pfeiffer BE, Nosyreva ED, Ronesi JA, Huber KM. Rapid translation of Arc/Arg3.1 selectively mediates mGluR-dependent LTD through persistent increases in AMPAR endocytosis rate. Neuron. 2008; 59:84–97. [PubMed: 18614031]

Wijetunge LS, Till SM, Gillingwater TH, Ingham CA, Kind PC. mGluR5 regulates glutamate-dependent development of the mouse somatosensory cortex. J Neurosci. 2008; 28:13028–13037. [PubMed: 19052194]

Xu J, Zhu Y, Contractor A, Heinemann SF. mGluR5 has a critical role in inhibitory learning. J Neurosci. 2009; 29:3676–3684. [PubMed: 19321764]

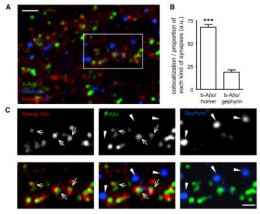

Figure 1. Aβ Oligomers Bind to Excitatory Synapses

(A) Labeling of Homer1b/c (red) and gephyrin (blue) in neurons incubated for 5 min with b-Aβo (500 nM). b-Aβo were labeled with streptavidin (green). Bar: 2 μm.

(B) Quantification of colocalization between b-Aβo and Homer or gephyrin normalized to the relative proportion of each kind of synapse (mean ± SEM; t test, ***$p < 0.0001$; $n = 13$ neurites).

(C) Detail of the square indicated in (A) showing in separate channels the immunoreactivity of Homer (arrows) and Gephyrin (triangles) and the labeling of b-Aβo (top panels). Bottom panels show merge images of b-Aβo and Homer (left) or Gephyrin (right) and the triple merging (center). Bar: 1 μm.

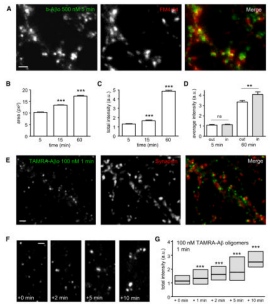

Figure 2. Aβ Oligomers Are Recruited in Aggregates by Means of Lateral Diffusion

(A) Labeling of b-Aβo (left) and synapses (FM4-64; middle) in living neurons after 5 min of b-Aβo application (500 nM). Right image shows the merging of both. Bar: 1 μm.

(B and C) Time dependence of b-Aβo cluster surface area (B) and total intensity (C) (mean ± SEM; 30 neurites; t test, ***$p < 0.0001$).

(D) b-Aβo average intensity at (in) or outside (out) synapses (mean ± SEM; 30 neurites; t test, **$p < 0.01$).

(E) Immunostaining of synapsin (middle) in neurons treated with TAMRA-Aβo (100 nM; left) for 1 min. Right image shows the merging of both. Bar: 1 μm.

(F and G) TAMRA-Aβo were applied for 1 min (100 nM) and neurons were observed at the indicated times after rinsing. Note that TAMRA-Aβo cluster fluorescence intensity increases progressively (quantified in G) even if there are no more oligomers in the cell medium. Bar: 1 μm.

(G) Quantification of TAMRA-Aβo fluorescence intensity (box: median, 25%, and 75% interquartiles; n = 676–2382 clusters; MW, ***$p < 0.0001$).

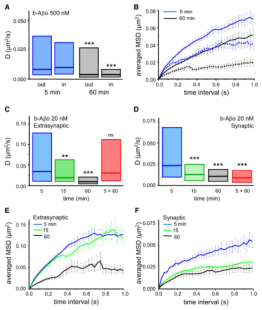

Figure 3. Aβ Oligomers Diffusing Laterally in the Plasma Membrane Are Slowed Down by Their Clustering

(A and B) Influence of incubation time on lateral diffusion properties of Aβo.

(A) Diffusion coefficient D for trajectories at (in) and outside (out) synapses after 5 min (blue boxes) or 60 min (white boxes) of Aβo application (median, 25%, and 75% interquartiles; KS test, ***$p < 0.0001$).

(B) Averaged MSD (mean ± SEM) plot for the same trajectories analyzed in (A), extrasynaptic (solid lines) or synaptic (broken lines).

(C and D) Diffusion coefficient D at extrasynaptic (C) and synaptic (D) membranes after continuous (5, 15, and 60 min) or pulsed (5 min and observed at 60 min; 5 + 60) b-Aβo application at low concentration (20 nM). Note that D decreases with incubation time and pulsed treatment has an effect only at synapses (median, 25%, and 75% interquartiles. KS test, **$p < 0.01$, ***$p < 0.0001$).

(E and F) Averaged MSD (mean ± SEM) plot of the trajectories analyzed in (C) and (D) for times of treatment 5, 15, and 60 min.

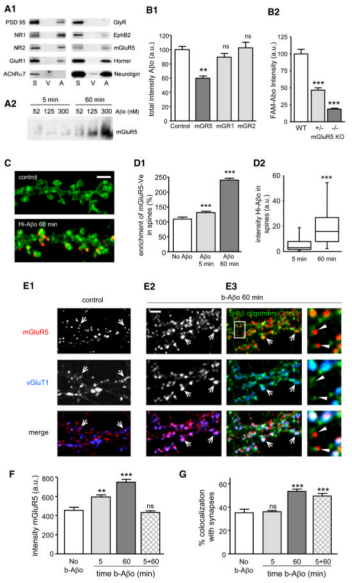

Figure 4. Aβ Oligomers Increase the Clustering of mGluR5 and Its Localization at Synapses

(A1) Coisolation of selected synaptic proteins from synaptosomes treated with Aβo (A) or vehicle (V) labeled with anti-Aβo (NU-2) and immunoprecipitated with anti-mouse IgG Dynabeads (S, total synaptosome protein; V and A, eluted fractions).

(A2) Western blot depicting the mGluR5 immunoreactivity in Triton-resistant DOC extractable fraction of neurons treated with Aβo at various concentrations (52, 125, and 300 nM) for 5 or 60 min.

(B1) Aβo total intensity in neurons preincubated with antibodies raised against an extracellular epitope of mGluR5 (mGR5), mGluR1 (mGR1), or mGluR2 (mGR2) prior to a treatment with 500 nM FAM-Aβo (mean ± SEM; n = 25–50 dendritic regions; ANOVA, **p < 0.001).

(B2) FAM-Aβo total intensity in neurons from wild-type (WT), heterozygous (+/−), or homozygous (−/−) mGluR5 KO mice (mean ± SEM; n = 64–175 dendritic regions; ANOVA, ***p < 0.001).

(C) Fluorescence of Venus-tagged mGluR5a (mGluR5-Ve; green) in control neurons or after 60 min of application of HiLyte555-tagged Aβo (Hi-Aβo; red). Bar: 2 μm.

(D1 and D2) Quantification of enrichment of mGluR5-Ve (D1) or total intensity of Hi- Aβo (D2) in spines in control (No Aβo) or Hi-Aβo-treated neurons (Aβo 5 or 60 min; median, 25%, and 75% IQR and 5%–95% confidence intervals; n = 194–776 spines on 25–43 cells; t test, ***p < 0.0001).

(E1–E3) Immunostaining of mGluR5 (top line) and synapses (vGluT1; middle line) in control (E1) or Aβo-treated (E2 and E3) neurons (b-Aβo 60 min; 500 nM). b-Aβo and mGluR5 staining were performed in nonpermeabilizing conditions. Arrows indicate synaptic mGluR5 clusters. Bar: 2 μm. (E1 and E2) Bottom line shows the merging of mGluR5 (red) and vGluT1 (blue). (E3) (Top) Merging of mGluR5 (red) and b-Aβo (green). (Center) Merging of b-Aβo (green) and vGluT1 (blue). (Bottom) Triple merging. Right column shows the magnification of the area indicated by the white rectangle. Triangles indicate mGluR5 clusters that colocalize with b-Aβo outside synapses.

(F) Quantification of total intensity of mGluR5 in the absence of b-Aβo (no b-Aβo) or after continuous (5 or 60 min) or pulsed (5 min observed at 60 min; 5 + 60) b-Aβo application (mean ± SEM; n = 25–50 cells; t test, **p < 0.001, ***p < 0.0001; ns, not significant).

(G) Colocalization of mGluR5 and vGluT1 immunoreactive clusters in the same conditions as in (F) (mean ± SEM; n = 25–50 cells; t test, ***p < 0.0001).

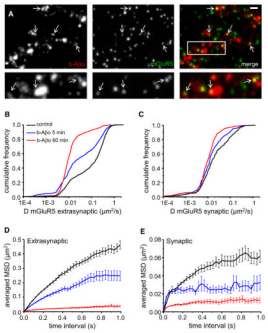

Figure 5. Aβ Oligomers Decrease mGluR5 Lateral Diffusion

(A) Labeling of b-Aβo (left) and mGluR5 (center) and merging of both (right) in living neurons. Cells were incubated first with b-Aβo for 60 min (500 nM) and then with anti-mGluR5 (10 min). Arrows indicate spots of mGluR5 (green) colocalized with b-Aβo (red). (Bottom) Higher magnification of the area indicated by the white rectangle. Bar: 1 μm (top) or 0.5 μm (bottom).

(B and C) Diffusion coefficients D for QD-mGluR5 trajectories on extrasynaptic (B) and synaptic (C) membranes in control cells (black) or after application of Aβo (b-Aβo; 500 nM) for 5 (blue) or 60 (red) min.

(D and E) Averaged MSD (mean ± SEM) plots of the same trajectories analyzed in (B) and (C) at extrasynaptic areas (D) and at synapses (E). Same color coding as in (B) and (C). Note that the amplitude of the effects depends on the duration of application.

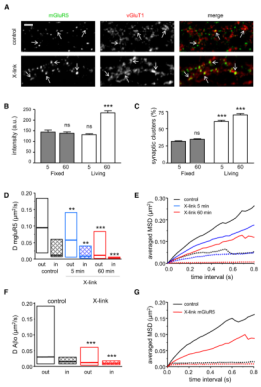

Figure 6. Effect of Crosslinking of mGluR5 on Its Distribution and Mobility

(A) Coimmunodetection of mGluR5 (left) and synapses (vGluT1; center) in control conditions or after 60 min of crosslinking of mGluR5 with an anti-mGluR5 antibody (X-link). Right images show the merging of both. Bar: 2 μm.

(B) Total fluorescence intensity of mGluR5 after 5 min (n = 17 cells) or 60 min (n = 15) of X-link (mean ± SEM). Neurons were incubated with streptavidin for the indicated times before (living) or after (fixed) fixation (mean ± SEM; t test, ***p < 0.0001; ns, not significant).

(C) Percentage of mGluR5 clusters colocalized with vGluT1 after 5 min (n = 17) or 60 min (n = 15) of X-link (mean ± SEM). Neurons were incubated as in (B) (t test, ***p < 0.0001; ns, not significant).

(D) Diffusion coefficient D for mGluR5 trajectories at (in) and outside (out) synapses in neurons without (black) or after 5 (blue) or 60 (red) min of X-link (median, 25%, and 75% interquartiles; KS test, **p < 0.001, ***p < 0.0001).

(E) Averaged MSD plots of the same trajectories analyzed in (D) (same color coding as in D) at (broken lines) and outside (solid lines) synapses.

(F and G) Neurons were treated first with unmodified Aβo (5 min, 20 nM) and mGluR5s were cross-linked with antibodies and streptavidin for 60 min. (F) Diffusion coefficient D for Aβo trajectories at (in) and outside (out) synapses in control cells (black) or after 60 min of crosslinking of mGluR5 (red) (median, 25%, and 75% interquartiles; KS test, ***p < 0.0001). (G) Average MSD plot of the same trajectories analyzed in (F) (same color coding as in F) at (broken lines) or outside (solid lines) synapses.

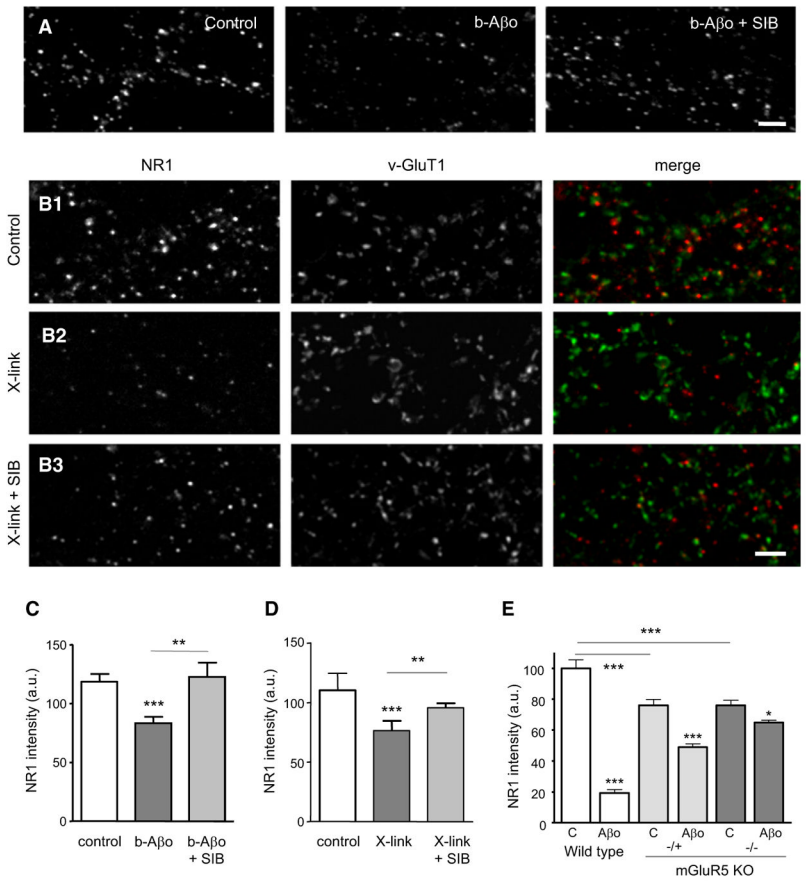

Figure 7. Decrease of NMDAR (NR1) at Synapses after Aβ Oligomer Treatment or Crosslinking of mGluR5

(A and B) NR1 fluorescence (NR1-IR) in control conditions, after Aβo application (A, Aβo) or mGluR5 crosslinking (B, X-link) for 60 min. NR1 staining was performed in nonpermeabilizing conditions. Mean ± SEM. Bar: 2 μm. (A) Note that Aβo-associated NR1-IR reduction is prevented by an mGluR5 antagonist (Aβo + SIB). (B) Double immunolocalization of NR1 and vGluT1 in control (B1), after mGluR5 X-link (B2) or after X-link together with SIB (B3).

(C) Quantification of NR1-IR intensity in the experiments illustrated in (A) (control: 118 ± 6 a.u.; b-Aβo 60 min: 83 ± 5; b-Aβo + SIB: 122 ± 11; t test, **p < 0.01, ***p < 0.001; n = 15 cells).

(D) Quantification of NR1-IR intensity in the experiments illustrated in (B) (control: 110 ± 14 a.u.; X-link 60 min: 76 ± 8; X-link + SIB: 95 ± 4; t test, **p < 0.001, ***p < 0.0001; n = 15 cells).

(E) Quantification of NR1-IR intensity in neurons from wild-type (WT), heterozygous (+/−), or homozygous (−/−) mGluR5 KO mice in control conditions (C) or after 3 hr of incubation with Aβo (mean ± SEM; n = 104–605 dendritic regions; ANOVA, *p < 0.05, ***p < 0.001).

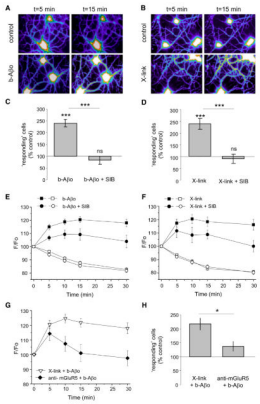

Figure 8. Aβ Oligomers and Crosslinking of mGluR5 Impact on Intracellular Calcium

Ca^{2+}_i monitored by fluorescence intensity of Fluo4AM on neurons treated with Aβo (A, C, and E) or after mGluR5 crosslinking (B, D, and F). Mean ± SEM.

(A and B) Examples of cells (Fluo4 intensity in pseudo-color).

(C and D) Percentage of "responding" neurons (that increased Fluo4AM intensity during the recordings) over control conditions. (C) Neurons treated with Aβo (500 nM) or Aβo and SIB (Aβo + SIB; t test, ***p > 0.0001; n = 16–22 fields of observation). (D) Neurons after mGluR5 X-link or after X-link and SIB (t test, ***p > 0.0001; n = 15–34 fields of observation).

(E and F) Fluo4AM fluorescence intensity over time (F/Fo; mean ± SEM) of cells where the intensity increased ("responding"; black symbols) or not ("not responding"; white symbols). (E) Cells treated with Aβo (circles) and with Aβo + SIB 1757 (squares) (n = 21–105 cells). (F) Cells after X-link of mGluR5 and without (circles) or with SIB 1757 (squares) (n = 27–127 cells).

(G and H) Neurons were treated for mGluR5 cross-linking and with Aβo (500 nM; X-link + Aβo) or they were incubated with an anti-mGluR5 antibody prior to Aβo application (anti-mGluR5 + Aβo). (G) Fluo4AM fluorescence intensity over time (F/Fo; mean ± SEM) of responding neurons treated with mGluR5 X-link + Aβo (black triangles) or with anti-mGluR5 antibody + Aβo (white triangles) (n = 44–62 cells). (H) Percentage of responding neurons treated as in (G) (percentage over control conditions; t test, p = 0.030; n = 10–20 fields of observation).

Table 1

Median D Values of mGluR5 or Aβo

Median D	**Extrasynaptic**		**Synaptic**	
(10^{-2} μm^2·sec^{-1})	mGluR5	Aβo	mGluR5	Aβo
Control *(n)*	14.48 (*900*)	n/a	1.48 (*368*)	n/a
5 min with 20 nM Aβo *(n)*	9.97 (*260*)**	3.41 (*279*)	1.80 (*65*)^{ns}	2.35 (*191*)
5 min with 500 nM Aβo *(n)*	2.02 (*597*)***	0.86 (*713*)	1.17 (*221*)*	1.02 (*609*)
15 min with 20 nM Aβo *(n)*	n/d	1.91 (*264*)	n/d	1.30 (*327*)
60 min with 20 nM Aβo *(n)*	1.03 (*413*)***	0.95 (*171*)	0.89 (*190*)***	1.07 (*176*)
60 min with 500 nM Aβo *(n)*	0.89 (*577*)***	0.41 (*195*)	0.95 (*241*)***	0.41 (*181*)

Summary table of median D values of mGluR5 or Aβo, in neurons in control conditions or treated with 20 nM or 500 nM Aβo. Controls correspond here to cells incubated for 60 min with the control solution (similar values were obtained when they were incubated for 5 min). Numbers in parentheses are the total number of trajectories. KS test,

* $p < 0.05$,

** $p < 0.01$,

*** $p < 0.0001$.

n/a, not applicable. n/d, no data; ns, not significant.

Table 2

Effect of Aβo on the Lateral Diffusion of Receptors

Median D	**Vehicle**		**60 min Aβo**	
(10^{-2} μm^2·sec^{-1})	extrasyn	syn	extrasyn	syn
mGluR5 *(n)*	14.48 (*900*)	1.48 (*368*)	0.89 (*577*)***	0.95 (*241*)***
AMPAR *(n)*	7.80 (*518*)	0.57 (*153*)	7.19 (*170*)^{ns}	1.08 (*156*)^{ns}
GABAR *(n)*	13.83 (*210*)	2.39 (*157*)	10.92 (*345*)***	3 (*236*)*

Median D values of the different receptors in control conditions (vehicle) or after 60 min of Aβo application (500 nM) at (syn) or outside (extrasyn) synapses. Numbers in parentheses are the total number of trajectories. KS test,

* $p < 0.05$,

*** $p < 0.0001$.

ns, not significant.

Table 3

Median D Values of mGluR5 or Aβo in Control Conditions or after Crosslinking of mGluR5

Median D	**Extrasynaptic**		**Synaptic**	
(10^{-2} $\mu m^2 \cdot sec^{-1}$)	mGluR5	Aβo	mGluR5	Aβo
Control *(n)*	8.91 (*284*)	3.00 (*263*)	1.46 (*104*)	1.51 (*167*)
5 min X-link *(n)*	5.75 (*169*)***	n/d	0.94 (*126*)***	n/d
60 min X-link *(n)*	1.13 (*447*)***	1.23 (*418*)***	0.32 (*163*)***	1.00 (*396*)***

Median D values of mGluR5 or Aβo (applied at 20 nM), in control conditions or after crosslinking of mGluR5. Numbers in parentheses are the total number of trajectories. KS test,

*** $p < 0.0001$.

n/d, no data.